LRH-1-mediated glucocorticoid synthesis in enterocytes protects against inflammatory bowel disease

Agnes Coste*, Laurent Dubuquoy*†, Romain Barnouin*, Jean-Sebastien Annicotte*, Benjamin Magnier*, Mario Notti‡, Nadia Corazza‡, Maria Cristina Antal§, Daniel Metzger*, Pierre Desreumaux†, Thomas Brunner‡, Johan Auwerx*§, and Kristina Schoonjans*¶

*Institut de Génétique et de Biologie Moléculaire et Cellulaire, Centre National de la Recherche Scientifique (CNRS), Institut National de la Santé et de la Recherche Médicale (INSERM), Université Louis Pasteur, 67404 Illkirch, France; †INSERM U795 Université de Lille 2 et Service des Maladies de l'Appareil Digestif et de la Nutrition, Hôpital Huriez, Centre Hospitalier Régional Universitaire Lille, 59037 Lille, France; ‡Division of Immunopathology, Institute of Pathology, University of Bern, 3010 Bern, Switzerland; and §Institut Clinique de la Souris, Génopole de Strasbourg, 67404 Illkirch, France

Edited by Philippa Marrack, National Jewish Medical and Research Center, Denver, CO, and approved June 25, 2007 (received for review March 15, 2007)

Liver receptor homolog-1 (LRH-1) is a nuclear receptor involved in intestinal lipid homeostasis and cell proliferation. Here we show that haploinsufficiency of LRH-1 predisposes mice to the development of intestinal inflammation. Besides the increased inflammatory response, LRH-1 heterozygous mice exposed to 2,4,6-trinitrobenzene sulfonic acid show lower local corticosterone production as a result of an impaired intestinal expression of the enzymes CYP11A1 and CYP11B1, which control the local synthesis of corticosterone in the intestine. Local glucocorticoid production is strictly enterocyte-dependent because it is robustly reduced in epithelium-specific LRH-1-deficient mice. Consistent with these findings, colon biopsies of patients with Crohn's disease and ulcerative colitis show reduced expression of LRH-1 and genes involved in the production of glucocorticoids. Hence, LRH-1 regulates intestinal immunity in response to immunological stress by triggering local glucocorticoid production. These findings underscore the importance of LRH-1 in the control of intestinal inflammation and the pathogenesis of inflammatory bowel disease.

Crohn's disease | inflammation | nuclear receptors | steroidogenesis | ulcerative colitis

Liver receptor homolog-1 (LRH-1) is a nuclear receptor whose expression is predominantly confined to the enterohepatic axis and the ovary (1). Previously recognized as an orphan receptor, phospholipids, including the phosphatidyl inositol second messengers, have been proposed as ligands for the human form (2–4). Although the role of LRH-1 in cholesterol and bile acid homeostasis is relatively well established (5–14), unanticipated actions of LRH-1 in the intestine have emerged, including control of cell renewal (15). This finding was shown to be the result of cross-talk between LRH-1 and the β-catenin pathway (15), through which LRH-1 contributes to tumorigenesis under pathophysiological conditions (16). In the same study, however, a potential inflammatory component of LRH-1-mediated tumor formation was evoked (16). Here we show that germ-line haploinsufficiency or somatic deficiency of LRH-1 in the intestinal epithelium predisposes mice to intestinal inflammation as a result of a defect in local glucocorticoid production. In colons from patients with inflammatory bowel disease (IBD), inflammation is inversely correlated with the expression of LRH-1 and genes involved in the production of glucocorticoids, suggesting that LRH-1 regulates intestinal immunity by triggering local glucocorticoid production. These findings indicate a protective role for LRH-1 against the onset of IBD.

Results and Discussion

***Lrh-1*$^{+/-}$ Mice Are Hypersensitive to Hapten-Induced Gut Inflammation.** The intestine is characterized by the presence of an elaborate immune system ensuring protective host defense. Chronic disorders of the bowel, such as Crohn's disease (CD) and ulcerative colitis (UC), are usually the result of an inappropriate regulation of the immune response leading to sustained inflammation and mucosal injury. Recently, a potential link between LRH-1 signaling and inflammation has been put forward in the intestine (16). This finding prompted us to investigate whether LRH-1 was involved in the pathogenesis of IBD. Contrary to the embryonic lethal phenotype of homozygous *Lrh-1*$^{-/-}$ mice, heterozygous *Lrh-1*$^{+/-}$ mice survive and have a normal lifespan (15). To study the role of LRH-1 in intestinal inflammation, we subjected *Lrh-1*$^{+/+}$ and *Lrh-1*$^{+/-}$ mice to 2,4,6-trinitrobenzene sulfonic acid (TNBS) treatment, a mouse colitis model that has many similarities with human IBD (17, 18). Intrarectal TNBS administration induced severe colitis in the colon of both *Lrh-1*$^{+/+}$ and *Lrh-1*$^{+/-}$ mice, but the colon of *Lrh-1*$^{+/-}$ mice appeared significantly more inflamed compared with control littermates as evidenced by the increased edema and vascular response (Fig. 1*A*). The higher degree of inflammation found in the colon of *Lrh-1*$^{+/-}$ mice was characterized by more necrotic regions and a higher level of neutrophilic infiltration [Fig. 1*B Middle* and supporting information (SI) Fig. 6]. Whereas no differences in lesion scores were detected under control conditions in mice from both genotypes (Fig. 1*B Top* and data not shown), *Lrh-1*$^{+/-}$ mice had more pronounced macro- and microscopic scores 48 h after a challenge with TNBS (Fig. 1*C*). Consistent with these observations, myeloperoxidase activity, a marker of neutrophil infiltration, was also significantly induced in the *Lrh-1*$^{+/-}$ mice (Fig. 1*C Right*). *Lrh-1*$^{+/+}$ and *Lrh-1*$^{+/-}$ mice were next subjected to dextran sodium sulfate (DSS) treatment, resulting in the induction of a less acute colitis, which allows the study of lesion healing. Also after DSS exposure, *Lrh-1*$^{+/-}$ mice showed a more severe inflammatory response (Fig. 1*B Bottom*). The colon weight/length ratio and the histological score were significantly increased in *Lrh-1*$^{+/-}$ mice (Fig. 1*D*), reflecting increased inflammation and decreased capacity of the epithe-

Author contributions: K.S. designed research; A.C., L.D., R.B., J.-S.A., B.M., M.N., and N.C. performed research; D.M. contributed new reagents/analytic tools; A.C., M.C.A., P.D., T.B., and J.A. analyzed data; and K.S. wrote the paper.

The authors declare no conflict of interest.

This article is a PNAS Direct Submission.

Abbreviations: CD, Crohn's disease; DSS, dextran sodium sulfate; IBD, inflammatory bowel disease; LRH-1, liver receptor homolog-1; TNBS, 2,4,6-trinitrobenzene sulfonic acid; UC, ulcerative colitis; vil, villin.

¶To whom correspondence should be addressed at: Institut de Génétique et de Biologie Moléculaire et Cellulaire, 1 Rue Laurent Fries, Parc d'Innovation, 67404 Illkirch, France. E-mail: schoonja@igbmc.u-strasbg.fr.

This article contains supporting information online at www.pnas.org/cgi/content/full/0702440104/DC1.

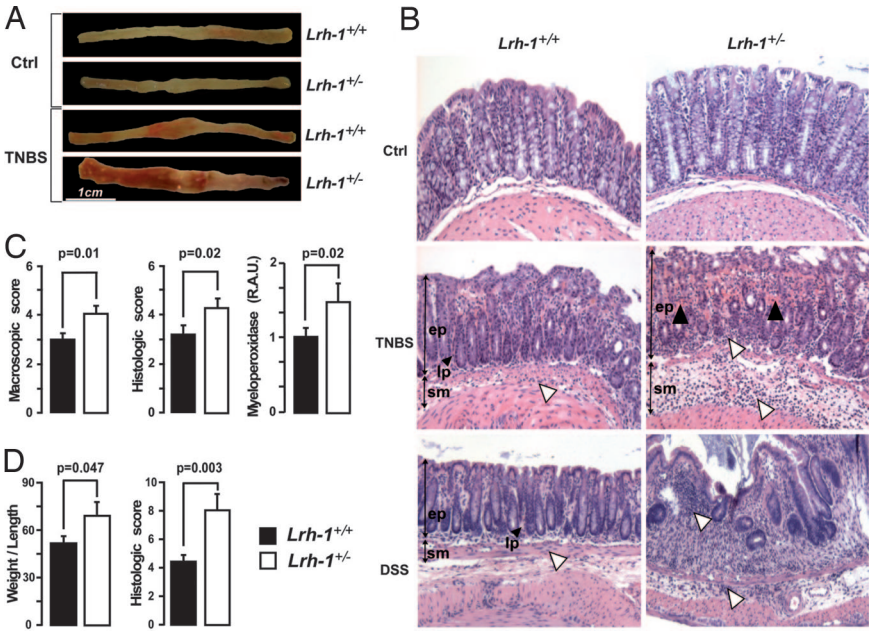

Fig. 1. *Lrh-1*$^{+/-}$ mice are more susceptible to TNBS- or DSS-induced colitis than their wild-type littermates. (*A*) Representative macroscopic view of the colon of *Lrh-1*$^{+/+}$ or *Lrh-1*$^{+/-}$ mice 48 h after vehicle (Ctrl) or TNBS administration. (*B*) Representative H&E staining of colon sections of *Lrh-1*$^{+/+}$ or *Lrh-1*$^{+/-}$ mice 48 h after vehicle (Ctrl) or TNBS administration and 12 days after DSS administration. TNBS induces thickening of the colon wall, with predominant inflammatory infiltrate (open arrowheads) present in the lamina propria (lp) and submucosa (sm) of TNBS-treated *Lrh-1*$^{+/-}$ mice. Compared with *Lrh-1*$^{+/+}$ mice, necrosis (filled arrowheads) is more severe in *Lrh-1*$^{+/-}$ mice, with necrotic regions detected in the colonic epithelium (ep). After DSS administration, colons of *Lrh-1*$^{+/+}$ mice were characterized by a mild inflammatory infiltrate (open arrowheads) and advanced crypt regeneration. In *Lrh-1*$^{+/-}$ mice, a massive infiltrate is associated with an important crypt loss and poor epithelium regeneration. (*C*) Macroscopic and histologic assessment of the colon of *Lrh-1*$^{+/+}$ ($n = 21$) or *Lrh-1*$^{+/-}$ ($n = 17$) mice 48 h after TNBS administration, using the Wallace and Ameho scores, respectively. Quantification of myeloperoxidase levels was performed by immunoblotting. (*D*) Assessment of colonic weight/length ratio and histological score of *Lrh-1*$^{+/+}$ ($n = 7$) and *Lrh-1*$^{+/-}$ ($n = 7$) mice after DSS-induced colitis.

lium to regenerate. Hence, these data suggest that the presence of LRH-1 protects the intestinal epithelium against inflammation in two independent models of induced colitis and confirms its role in epithelium regeneration.

We next analyzed the expression of some key inflammatory genes in the colon of TNBS- or DSS-exposed animals (Fig. 2 *A* and *B*). As expected, gene expression levels of the proinflammatory cytokines TNF-α, IL-1β, and IL-6 were significantly induced in the colon of *Lrh-1*$^{+/+}$ mice 6 or 48 h after TNBS instillation (Fig. 2*A* and SI Fig. 7) or 12 days after DSS

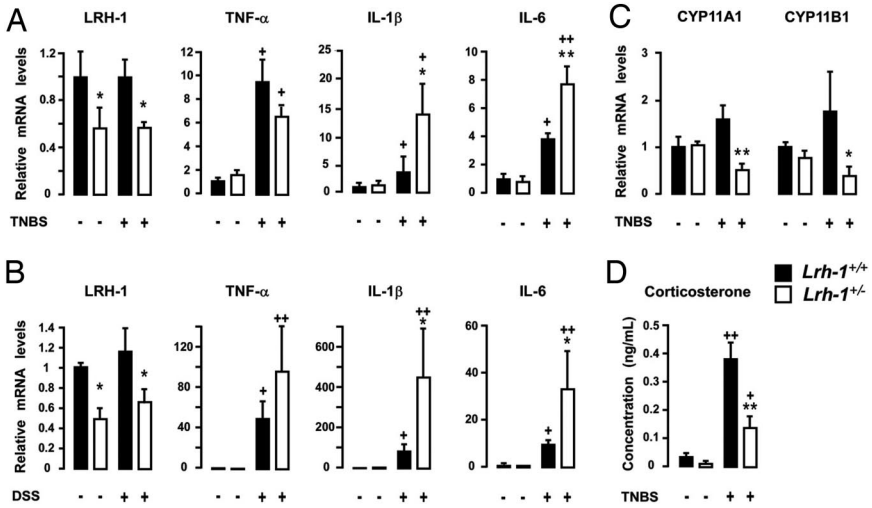

Fig. 2. Exaggerated inflammatory response in *Lrh-1*$^{+/-}$ mice is closely associated with decreased intestinal corticosterone production. (*A* and *B*) Effect of LRH-1 haplodeficiency on TNF-α, IL-1β, and IL-6 gene expression in *Lrh-1*$^{+/+}$ (filled bars) or *Lrh-1*$^{+/-}$ (open bars) mice after TNBS- or DSS-induced colitis. LRH-1, TNF-α, IL-1β, and IL-6 mRNA levels in the colon of *Lrh-1*$^{+/+}$ or *Lrh-1*$^{+/-}$ mice challenged with vehicle or TNBS for 48 h (*A*) or 12 days after vehicle or DSS administration (*B*). +, $P < 0.05$ and ++, $P < 0.01$ depict significant differences between untreated and treated groups from the same genotype; *, $P < 0.05$ and **, $P < 0.01$ depict significant differences between genotypes receiving the same treatment. (*C* and *D*) mRNA levels of steroidogenic enzymes CYP11A1 and CYP11B1 (*C*) and *in situ*-produced glucocorticoids (*D*) in colon biopsies of *Lrh-1*$^{+/+}$ (filled bars) or *Lrh-1*$^{+/-}$ (open bars) mice killed 24 h after vehicle or TNBS instillation. *, $P < 0.05$; **, $P < 0.01$.

administration (Fig. 2*B*). We then investigated whether the exacerbated inflammation observed in *Lrh-1*$^{+/-}$ mice after TNBS or DSS was paralleled with an altered gene expression pattern of the three cytokines studied. Although the expression of the TNF-α mRNA in wild-type animals was significantly induced by TNBS (Fig. 2*A*) and DSS (Fig. 2*B*), it did not seem to be affected by the loss of one *Lrh-1* allele. By contrast, IL-1β and IL-6 mRNA levels were significantly elevated in *Lrh-1*$^{+/-}$ mice after TNBS (Fig. 2*A*) and DSS (Fig. 2*B*) treatment. Although these data are consistent with two recent reports implicating LRH-1 as a negative regulator of the acute-phase response in the liver (19, 20), it is perhaps less evident to directly link the exaggerated inflammatory response to the decreased tumorigenesis reported earlier in *Lrh-1*$^{+/-}$ genetic and chemical models for colon cancer (16). Even if these cancer models are difficult to compare with the colitis model used in this study, it may be that the stimulatory role of LRH-1 in β-catenin/Tcf4-mediated cell renewal, which is dampened in the germ-line *Lrh-1*$^{+/-}$ mice, could affect the efficacy of epithelial repair after hapten-induced epithelial damage and ultimately contribute to the effects on mucosal inflammation.

Increased Inflammatory Response in TNBS-Treated *Lrh-1*$^{+/-}$ Mice Is Associated with Decreased Intestinal Corticosterone Production. Glucocorticoids are potent immunosuppressive agents that limit inflammation by both inhibiting the expression of proinflammatory cytokines by interference with NF-κB and AP-1 and inducing the expression of antiinflammatory proteins (21). Because LRH-1 was recently identified to control local glucocorticoid production in the intestinal mucosa (22), we analyzed whether the increased inflammation observed in *Lrh-1*$^{+/-}$ mice after TNBS administration was correlated with an altered gene expression pattern of CYP11A1 and CYP11B1. These two genes encode for the P450 cholesterol side-chain cleavage enzyme and P450C11 of the cytochrome P450 gene family, and both are involved in the synthesis of corticosterone, the bioactive form of glucocorticoids. Interestingly, mRNA levels of both CYP11A1 and CYP11B1 were robustly reduced in the colon of *Lrh-1*$^{+/-}$ mice 24 h after TNBS instillation (Fig. 2*C*). Consistent with these findings, a marked reduction in the release of local corticosterone could be observed (Fig. 2*D*), indicating that TNBS-induced production of intestinal glucocorticoids is critically dependent on LRH-1 expression.

Conditional Deletion of LRH-1 in the Intestinal Epithelium Compromises Synthesis of Local Glucocorticoids and Aggravates Colitis. LRH-1 and the steroidogenic enzymes CYP11A1 and CYP11B1 are both expressed in the crypt region of the intestinal epithelial layer (15, 23). Upon injection of anti-CD3 antibody, LRH-1, CYP11A1, and CYP11B1 become highly induced (23). Because TNBS or DSS treatment does not increase LRH-1 mRNA levels (Fig. 2*A* and *B*), it is likely that the activation of the steroidogenic genes by these chemical agents may not only be controlled by LRH-1, but also by other signals from epithelial cells or, alternatively, by signals derived from local immune cells recruited after inflammatory insult. Germ-line *Lrh-1*$^{+/-}$ mice express lower levels of LRH-1 in each of the cell types that express LRH-1. Consequently, this mouse model cannot exclude a potential contribution of nonepithelial cells, such as immune cells, to the observed intestinal phenotype. To unequivocally determine the cellular origin that accounts for the observed increased inflammation and reduced corticosterone production in the colon, we generated mice that carry conditional *Lrh-1* alleles (*Lrh-1*$^{L2/L2}$ mice) by using classical gene targeting (Fig. 3 *A–C*). To generate temporally and spatially controlled mouse mutants for the *Lrh-1* gene in the progenitor and epithelial cells of the crypts, mice carrying the floxed *Lrh-1*^{L2} alleles were crossed with transgenic mice that express the Cre-ER^{T2} recombinase under the control of the mouse villin (vil) promoter (24). Vil-Cre-ER^{T2}/*Lrh-1*$^{L2/L2}$ bigenic mice were then injected with vehicle or tamoxifen to induce Cre-mediated recombination of the floxed *Lrh-1* alleles in the intestinal epithelium. Three weeks after tamoxifen injection, effective and selective recombination of the *Lrh-1* locus could be detected along the gastrointestinal tract, but not in the pancreas or liver, which are other tissues of the enterohepatic axis that express LRH-1 (Fig. 3*D*). As reported earlier (24), a weak recombination in the kidney could be observed in the tamoxifen-treated vil-Cre-ER^{T2}/*Lrh-1*$^{L2/L2}$ mice, but this did not interfere with the tissue-specificity of the mouse model because the kidney does not express LRH-1 (25). In the colon of the vil-Cre-ER^{T2}/*Lrh-1*$^{L2/L2}$ mice, LRH-1 mRNA and protein levels were almost undetectable after tamoxifen (Fig. 3 *E* and *F*). These mice, referred to as *Lrh-1*$^{vil-/-}$ mice, were then treated with vehicle or TNBS for 24 h and analyzed. In the absence of TNBS, deletion of LRH-1 in the intestinal epithelium did not affect gut morphology (Fig. 4*A Upper*). Administration of TNBS, however, triggered a colonic inflammation that was more pronounced and extensive in *Lrh-1*$^{vil-/-}$ mice. Most of these colons studied also displayed severe lesions in which necrosis was highly advanced (Fig. 4*A Lower*). In addition, *Lrh-1*$^{vil-/-}$ mice had more pronounced macro- and microscopic scores, as well as increased myeloperoxidase activity 24 h after a challenge with TNBS (Fig. 4*B*). Consistent with these observations, IL-1β and IL-6 mRNA levels were significantly induced in *Lrh-1*$^{vil-/-}$ mice after TNBS administration (Fig. 4*C*). Interestingly, the absence of LRH-1 in the epithelial cells of the intestinal epithelium was again correlated with substantially reduced levels of CYP11A1 and CYP11B1 mRNA (Fig. 4*D*) and corticosterone in the colon (Fig. 4*E*). Altogether, these results corroborate the previous findings identifying CYP11A1 and CYP11B1 as targets of LRH-1 and unequivocally demonstrate that *in vivo* the regulatory effects of LRH-1 on the expression of these steroidogenic genes are primarily confined to the intestinal epithelium.

Severity of Inflammation in Colons of IBD Patients Is Inversely Correlated with LRH-1 and Local Glucocorticoid Synthesis. Based on the observation that both germ-line *Lrh-1*$^{+/-}$ and somatic *Lrh-1*$^{vil-/-}$ mice are more susceptible to the development of colitis, we next analyzed the expression of LRH-1 in colon biopsies from control subjects and biopsies taken from healthy and inflamed mucosa in both CD and UC patients. The inflamed intestine of both IBD pathologies showed in each case an increase in the proinflammatory markers TNF-α, IL-1β, and IL-6 relative to macroscopically and histologically healthy intestine (Fig. 5*A*). Most intriguingly, LRH-1 mRNA levels were robustly decreased in inflamed colon biopsies of both CD and UC patients, compared with biopsies of healthy-looking mucosa (Fig. 5*B*). Because values were normalized to the epithelial marker cytokeratin 20 (26), the decrease in expression was not the result of increased necrosis that leads to loss of intestinal epithelium. This finding was further reflected by the reduction of both LRH-1 isoforms in the inflammatory lesions of patients with UC and CD (Fig. 5 *C* and *D*). Therefore, these mRNA and protein data prove that human intestinal inflammation occurring in both CD and UC is associated with a specific reduction in LRH-1 expression. Consistent with the expression data in both mouse models, mRNA levels of CYP11A1 and CYP11B1 were robustly decreased in inflamed colon biopsies of CD and UC patients compared with healthy biopsies of IBD patients and controls (Fig. 5*B*), suggesting that this mechanism can contribute to the pathogenesis of IBD in humans.

In summary, our data demonstrate that the reduction of LRH-1 increases the susceptibility of mice to compound-induced experimental colitis. Furthermore, patients with CD and UC express reduced amounts of LRH-1 mRNA and protein in

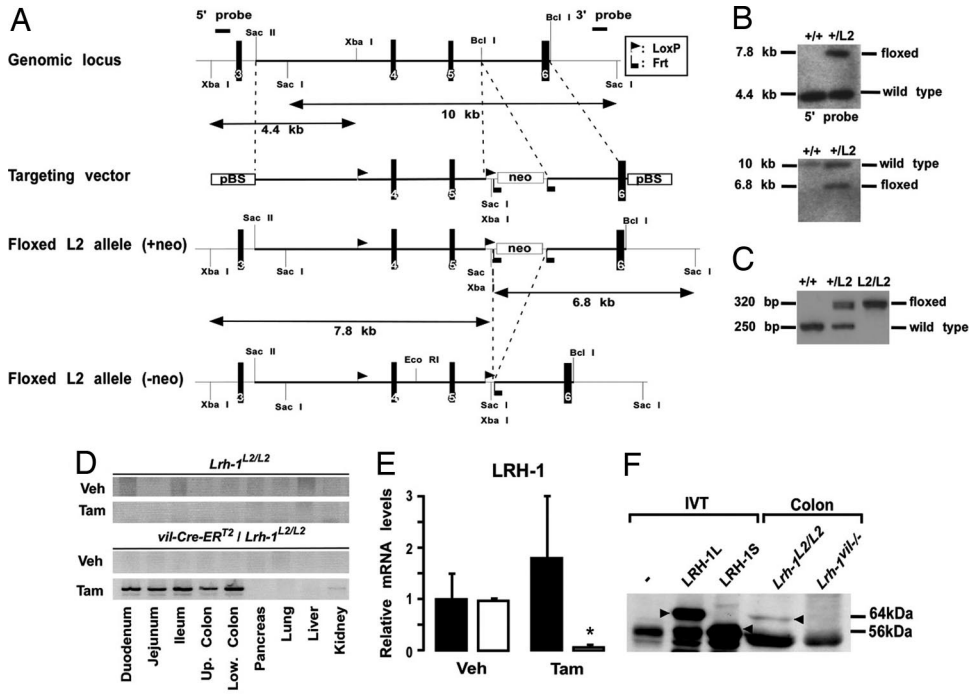

Fig. 3. Gene targeting and tamoxifen-induced deletion of the *Lrh-1* gene in the intestinal epithelium. (*A*) Restriction maps of the *Lrh-1* genomic locus, targeting vector, floxed allele +neo, and floxed allele −neo. The indicated probes (5′ probe and 3′ probe) were used to assess recombination events. Boxes represent the respective exons. (*B*) Southern blot analysis revealing homologous recombination in ES cells electroporated with targeting vector. DNA derived from ES cells was digested with XbaI or SacI. Hybridizing fragments of wild-type (+/+) and floxed (+/L2) alleles to the 5′ probe or the 3′ probe, and their respective sizes, are indicated. (*C*) Recombination of loxP sites as demonstrated with PCR analysis of genomic DNA from ES cells. Size of PCR products in floxed and wild type are indicated. (*D–F*) Conditional loss of LRH-1 in intestinal epithelium (*Lrh-1*$^{vil-/-}$) after tamoxifen-induced recombination in *Lrh-1*$^{L2/L2}$ mice mated to vil-Cre-ER^{T2} transgenic mice (vil-Cre-ER^{T2}/*Lrh-1*$^{L2/L2}$). (*D*) Analysis of recombination of *Lrh-1* locus by PCR on genomic DNA isolated from various tissues of *Lrh-1*$^{L2/L2}$ and vil-Cre-ER^{T2}/*Lrh-1*$^{L2/L2}$ mice treated with olive oil/ethanol (10:1) (Veh) or tamoxifen (Tam). (*E*) LRH-1 mRNA levels in the colon of *Lrh-1*$^{L2/L2}$ mice (filled bars, $n = 4$) and vil-Cre-ER^{T2}/*Lrh-1*$^{L2/L2}$ mice (open bars, $n = 4$) as determined by quantitative RT-PCR analysis. *, $P < 0.05$. (*F*) LRH-1 immunoblotting performed on protein extracts of nuclear membrane and chromatin fraction from colon of *Lrh-1* $^{L2/L2}$ and vil-Cre-ER^{T2}/*Lrh-1* $^{L2/L2}$ mice (LRH-1$^{vil-/-}$). Specific bands corresponding to long (LRH-1L) and short (LRH-1S) isoforms of mouse LRH-1 are indicated by arrowheads.

inflamed intestinal biopsies, suggesting that the presence of LRH-1 could protect against the onset of IBD. This protective effect of LRH-1 against intestinal inflammation is intimately linked with its commanding role on glucocorticoid synthesis in the intestinal epithelium as concluded from our studies by using a mouse model that lacks LRH-1 expression specifically in the intestinal epithelium. These observations warrant a thorough analysis of the implication of LRH-1-mediated signaling pathways in the pathogenesis, prevention, and treatment of IBD.

Materials and Methods

Generation of LRH-1 Mutant Models. *Lrh-1*$^{+/-}$ mice have been described earlier (15). To generate LRH-1 floxed (*Lrh-1*$^{L2/L2}$) mice, genomic DNA covering the *Lrh-1* locus was amplified from the 129Sv strain by using high-fidelity PCR. The resulting DNA fragments were assembled into the targeting vector that, after linearization by NotI, was electroporated into 129Sv ES cells. G418-resistant colonies were selected and analyzed for homologous recombination by PCR and Southern blot hybridization. For the PCR screening strategy, primers ACE225 5′-GTCATAGGGAGTCAGGATACCATGG-3′, ACE228 5′-GTTCTGACCACTTTCATCTCCTCACG-3′, ACE229 5′-CTCAACTGCCGAAGAATGCTGCGG-3′, and ACE231 5′-GTTAGCAATTTGGCAGATTTACGC-3′ were used. Positive clones were verified by Southern blot hybridization. Therefore, genomic DNA was prepared from ES cells, digested with XbaI or SacI, subjected to electrophoresis, and transferred to a positively charged nylon transfer membrane (Amersham Biosciences, Saclay, France). A 0.5-kb DNA fragment (NotI–NheI) located between exons 6 and 7 (3′ probe) and a 0.5-kb DNA fragment (NotI–SacII) placed between exons 2 and 3 (5′ probe) were used as probes. The karyotype was verified, and several correctly targeted ES cell clones were injected into blastocysts from C57BL/6J mice. These blastocysts were transferred into pseudopregnant females, resulting in chimeric offspring that were mated to female C57BL/6J mice that express the Flp recombinase under the control of the ubiquitous CMV promoter (27). Offspring that transmitted the mutated allele, in which the selection marker was excised and that lost the Flp transgene (*Lrh-1*$^{+/L2}$ mice), were then selected and used for systematic backcrossing with C57BL/6J mice to generate congenic *Lrh-1* floxed mouse lines. A PCR genotyping strategy was subsequently used to identify *Lrh-1*$^{+/+}$, *Lrh-1*$^{+/L2}$, and *Lrh-1*$^{L2/L2}$ mice. To generate tamoxifen-inducible, enterocyte-specific mutant (*Lrh-1*$^{vil-/-}$) mice, *Lrh-1*$^{L2/L2}$ mice were mated with vil-Cre-ER^{T2} C57BL/6J mice. Vil-Cre-ER^{T2}/*Lrh-1*$^{L2/+}$ mice, heterozygous for the floxed *Lrh-1* allele, were selected and subsequently intercrossed to generate premutant vil-Cre-ER^{T2}/*Lrh-1*$^{L2/L2}$ mice. At least two more rounds of breeding were required to generate age- and sex-matched mice for experimental cohorts. Recombination of floxed alleles was induced by tamoxifen treatment (1-mg i.p. injection during 4 consecutive days).

Animal Procedures. Animal experiments were approved by the local ethics committee and performed according to European Union governmental guidelines. Mice were group-housed and accustomed to a 12-h light/dark cycle with free access to standard mouse chow (D03; Scientific Animal Food and Engineering,

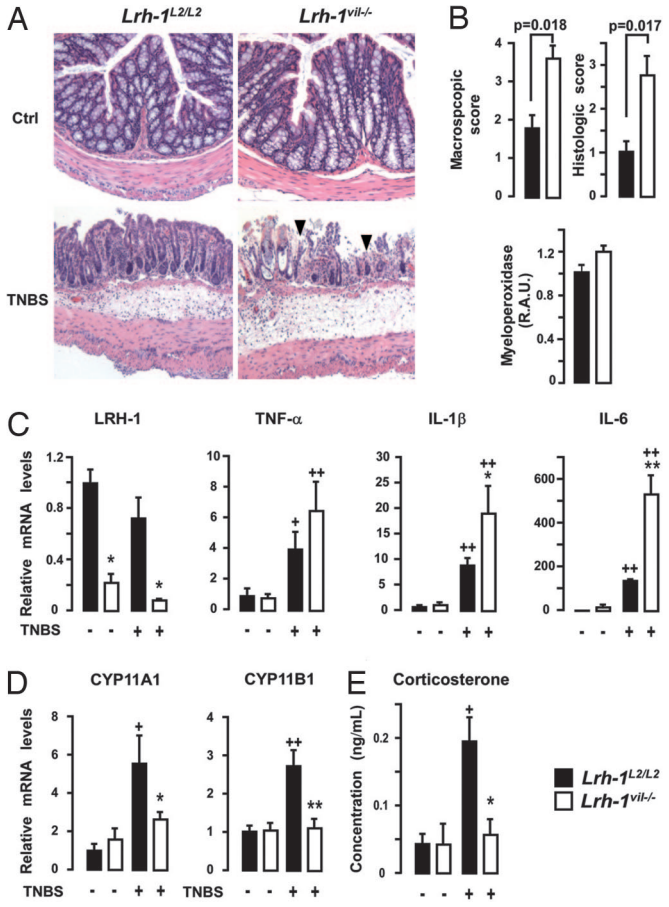

Fig. 4. TNBS-induced intestinal glucocorticoid production is impaired in enterocyte-specific LRH-1-deficient mice and leads to severe colitis. (*A*) H&E sections from control (*Lrh-1*$^{L2/L2}$) or mutant (*Lrh-1*$^{vil-/-}$) colons 24 h after vehicle (Ctrl) or TNBS administration. Filled arrowheads depict high-degree of necrosis. (Magnification: ×50.) (*B*) Macroscopic and histological assessment of the colon from *Lrh-1*$^{L2/L2}$ or *Lrh-1*$^{vil-/-}$ mice 24 h after TNBS administration. Quantification of myeloperoxidase levels was performed by immunoblotting. (*C*) LRH-1, TNF-α, IL-1β, and IL-6 mRNA levels in the colon of *Lrh-1*$^{L2/L2}$ (filled bars, $n = 7$) and *Lrh-1*$^{vil-/-}$ (open bars, $n = 7$) mice challenged with vehicle or TNBS for 24 h. +, $P < 0.05$ and ++, $P < 0.01$ depict significant differences between untreated and treated groups from the same genotype; *, $P < 0.05$ and **, $P < 0.01$ depict significant differences between genotypes receiving the same treatment. (*D* and *E*) mRNA levels of the steroidogenic genes CYP11A1 and CYP11B1 (*D*) and corticosterone production (*E*) in the colon biopsies of *Lrh-1*$^{L2/L2}$ (filled bars, $n = 7$) and *Lrh-1*$^{vil-/-}$ (open bars, $n = 7$) mice challenged with vehicle or TNBS for 24 h.

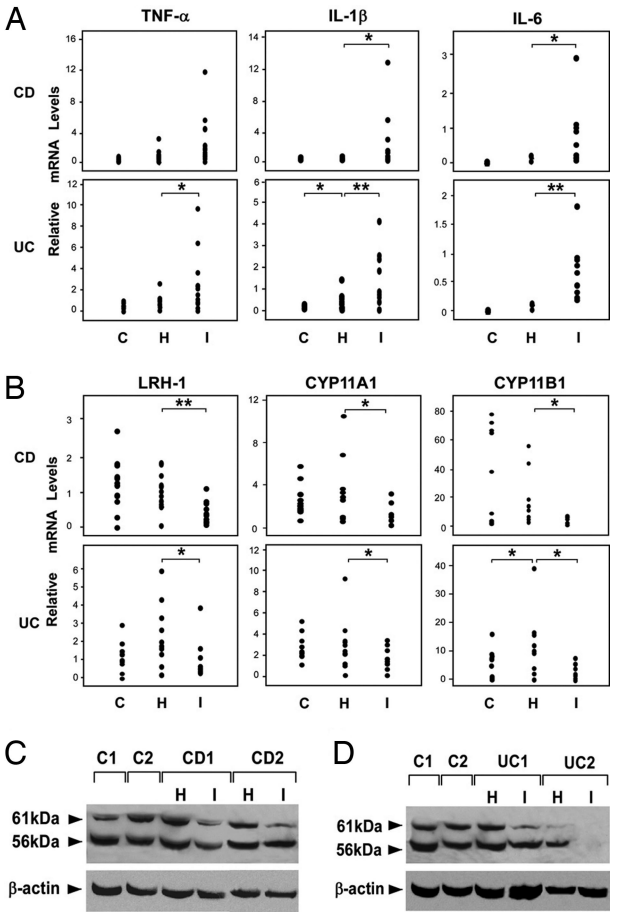

Fig. 5. Inflammation in colons of IBD patients is inversely correlated with LRH-1 and downstream targets required for local glucocorticoid synthesis. (*A* and *B*) Gene expression profiles of inflammation markers TNF-α, IL-1β, and IL-6 (*A*) and LRH-1, CYP11A1, and CYP11B1 (*B*) mRNA in colon biopsies of control subjects (C) ($n = 12$) or in healthy (H) ($n = 12$) or inflamed (I) ($n = 12$) mucosa of patients with CD or UC. *, $P < 0.05$; **, $P < 0.01$. (*C* and *D*) Representative immunoblots of CD ($n = 2$) (*C*) and UC ($n = 2$) (*D*) patients showing that the isoforms hLRH-1a (61 kDa) and hLRH-1b (56 kDa) are specifically decreased in the inflamed (I) parts of the colon compared with the healthy (H) part of the colon. No difference between the healthy-looking part of the colon (H) and the colon of control subjects (C) could be observed. β-actin was used as an internal loading control.

Villemoisson sur Orge, France) and tap water. For induction of TNBS colitis, anesthetized mice were given an intrarectal injection of 40 μl of a 150 mg/kg TNBS solution (Fluka Chemical, Ronkonkoma, NY) dissolved in 0.9% NaCl and mixed with an equal volume of 50% ethanol. Control mice received 50% ethanol intrarectally. In the enterocyte-specific LRH-1 control and mutant mice, TNBS was administered 3 weeks after tamoxifen injection. Animals were killed by CO_2 asphyxiation 24 or 48 h after TNBS administration. DSS colitis was induced as described (11). Briefly, 2.5% of DSS (MP Biochemicals, Irvine, CA) was added to the drinking water of mice. *Lrh-1*$^{+/-}$ mice and their wild-type littermates were exposed to DSS for 5 days and killed after 1 week (day 12). Body weight and rectal bleeding were monitored each day during the experiment. After the mice were killed, colons were measured and weighed, and macroscopic features were scored. The gastrointestinal tract was removed, washed with PBS, and prepared for RNA and protein extraction or morphological analysis.

Human Subjects. The study was approved by the institutional review board at the Centre Hospitalier Régional Universitaire of Lille, and patients gave informed consent. Colon biopsies were obtained from inflamed and macroscopically/histologically healthy mucosa from 12 UC patients (6 females and 6 males; mean age 43 years, range 28–51 years) and 12 CD patients (10 females and 2 males; mean age 31 years, range 18–48 years). The diagnoses of UC and CD were established by using standard criteria, and the mean durations of the diseases were 5.2 ± 2.3 and 7.0 ± 3.6 years, respectively. Patients did not receive any immunosuppressive or steroid treatments at the time of study. As controls, colon biopsies were taken from 12 patients with unrelated intestinal disorders (6 females and 6 males; mean age 59 years, range 30–83 years). Colon biopsy specimens were of similar size (mean weight 4 ± 1 mg) and taken with the same endoscopic forceps. Biopsies were immediately frozen in liquid nitrogen and stored at −80°C until analysis.

Macroscopic and Histologic Analyses. Colons from mice challenged with TNBS or DSS were examined under a dissecting microscope (×5) to evaluate the macroscopic lesions according to the Wallace criteria (28). Standardized colon specimens were harvested 1 cm above the anal canal. One part was fixed overnight in 4% paraformaldehyde and embedded in paraffin; 5-μm sections of mouse colon were stained with H&E and scored according to the Ameho criteria (29). The other parts of the colon were used for quantification of mRNA and protein levels.

RNA and Protein Expression Analyses. RNA preparation and quantitative RT-PCR analysis was performed as described (15). cDNA was synthesized by using the SuperScript System (Invitrogen, Carlsbad, CA) and random hexamer primers. Quantitative RT-PCR was performed by using LightCycler FastStart DNA Master SYBR Green I from Roche Diagnostics (Indianapolis, IN) according to the manufacturer's protocol. Primer sets used for mouse and human studies are listed in SI Table 1. Primers for β-actin, 18S, or cytokeratin 20, which is a marker for epithelial cells, were used as internal controls.

Measurement of Intestinal Corticosterone Synthesis. Corticosterone synthesis in the intestinal mucosa of TNBS-challenged mice was assessed as described (23). Twenty-four hours after the induction of TNBS colitis, mice were killed and colons were isolated, washed, and cultured for 6 h in the absence or presence of 200 μg/ml metyrapone, an agent blocking the activity of the corticosterol-synthesizing enzymes P450C11 and 11β-HSD1. After incubation, cell-free supernatant was harvested, and corticosterone was measured by radioimmunoassay (ICN Pharmaceuticals, Costa Mesa, CA). To correct for variable contamination with serum glucocorticoids, results were expressed as the difference between samples cultured with and without metyrapone.

Western Blot Analysis. Total or nuclear protein lysates were extracted following standard procedures. After protein transfer, membranes were incubated overnight at 4°C with a rabbit polyclonal antimyeloperoxidase (Dako, Fort Collins, CO) or an anti-LRH-1 antibody directed against the mouse C-terminal peptidic region VNGDVPYNNLLIEMLHAKR and then for 1 h at 21°C with a peroxidase conjugate secondary antibody. Membranes were washed, and proteins were visualized with the ECL kit (Amersham Pharmacia Biotech, Chalfont St. Giles, U.K.).

Statistics. Except stated otherwise, results are expressed as mean ± SEM. Differences between groups were calculated by unpaired two-tailed Student's t test and considered statistically significant when $P \leq 0.05$.

We thank A. Jauffre, A. Auburtin, and E. Garo for technical assistance. This work was supported by Centre National de la Recherche Scientifique, Institut National de la Santé et de la Recherche Médicale (INSERM), Université Louis Pasteur, Hôpitaux Universitaires de Strasbourg ACI Grant 03-2488, Association pour la Recherche sur le Cancer (ARC) (K.S.), Crohn's and Colitis Foundation and Swiss National Science Foundation (T.B.), INSERM grants (to A.C., L.D., and R.B.), and ARC fellowships (to J.-S.A. and B.M.). K.S. is a recipient of an INSERM Contrat d'Interface.

1. Fayard E, Auwerx J, Schoonjans K (2004) *Trends Cell Biol* 14:250–260.
2. Krylova IN, Sablin EP, Moore J, Xu RX, Waitt GM, MacKay JA, Juzumiene D, Bynum JM, Madauss K, Montana V, *et al*. (2005) *Cell* 120:343–355.
3. Ortlund EA, Lee Y, Solomon IH, Hager JM, Safi R, Choi Y, Guan Z, Tripathy A, Raetz CR, McDonnell DP, *et al*. (2005) *Nat Struct Mol Biol* 12:357–363.
4. Wang W, Zhang C, Marimuthu A, Krupka HI, Tabrizizad M, Shelloe R, Mehra U, Eng K, Nguyen H, Settachatgul C, *et al*. (2005) *Proc Natl Acad Sci USA* 102:7505–7510.
5. Nitta M, Ku S, Brown C, Okamoto AY, Shan B (1999) *Proc Natl Acad Sci USA* 96:6660–6665.
6. Lu TT, Makishima M, Repa JJ, Schoonjans K, Kerr TA, Auwerx J, Mangelsdorf DJ (2000) *Mol Cell* 6:507–515.
7. Goodwin B, Jones SA, Price RR, Watson MA, McKee DD, Moore LB, Galardi C, Wilson JG, Lewis MC, Roth ME, *et al*. (2000) *Mol Cell* 6:517–526.
8. del Castillo-Olivares A, Gil G (2000) *J Biol Chem* 275:17793–17799.
9. Luo Y, Liang CP, Tall AR (2001) *J Biol Chem* 276:24767–24773.
10. Inokuchi A, Hinoshita E, Iwamoto Y, Kohno K, Kuwano M, Uchiumi T (2001) *J Biol Chem* 276:46822–46829.
11. Schoonjans K, Annicotte JS, Huby T, Botrugno OA, Fayard E, Ueda Y, Chapman J, Auwerx J (2002) *Embo Rep* 3:1181–1187.
12. Fayard E, Schoonjans K, Annicotte JS, Auwerx J (2003) *J Biol Chem* 278:35725–35731.
13. Chen F, Ma L, Dawson PA, Sinal CJ, Sehayek E, Gonzalez FJ, Breslow JL, Ananthanarayanan M, Shneider BL (2003) *J Biol Chem* 278:19909–19916.
14. Freeman LA, Kennedy A, Wu J, Bark S, Remaley AT, Santamarina-Fojo S, Brewer HB, Jr (2004) *J Lipid Res* 45:1197–1206.
15. Botrugno OA, Fayard E, Annicotte JS, Haby C, Brennan T, Wendling O, Tanaka T, Kodama T, Thomas W, Auwerx J, Schoonjans K (2004) *Mol Cell* 15:499–509.
16. Schoonjans K, Dubuquoy L, Mebis J, Fayard E, Wendling O, Haby C, Geboes K, Auwerx J (2005) *Proc Natl Acad Sci USA* 102:2058–2062.
17. Strober W, Fuss IJ, Blumberg RS (2002) *Annu Rev Immunol* 20:495–549.
18. Wakefield AJ, Sawyerr AM, Dhillon AP, Pittilo RM, Rowles PM, Lewis AA, Pounder RE (1989) *Lancet* 2:1057–1062.
19. Venteclef N, Smith JC, Goodwin B, Delerive P (2006) *Mol Cell Biol* 26:6799–6807.
20. Venteclef N, Delerive P (2007) *J Biol Chem* 282:4393–4399.
21. Rhen T, Cidlowski JA (2005) *N Engl J Med* 353:1711–1723.
22. Mueller M, Cima I, Noti M, Fuhrer A, Jakob S, Dubuquoy L, Schoonjans K, Brunner T (2006) *J Exp Med* 203:2057–2062.
23. Cima I, Corazza N, Dick B, Fuhrer A, Herren S, Jakob S, Ayuni E, Mueller C, Brunner T (2004) *J Exp Med* 200:1635–1646.
24. el Marjou F, Janssen KP, Chang BH, Li M, Hindie V, Chan L, Louvard D, Chambon P, Metzger D, Robine S (2004) *Genesis* 39:186–193.
25. Bookout AL, Jeong Y, Downes M, Yu RT, Evans RM, Mangelsdorf DJ (2006) *Cell* 126:789–799.
26. Moll R, Zimbelmann R, Goldschmidt MD, Keith M, Laufer J, Kasper M, Koch PJ, Franke WW (1993) *Differentiation* 53:75–93.
27. Rodriguez CI, Buchholz F, Galloway J, Sequerra R, Kasper J, Ayala R, Stewart AF, Dymecki SM (2000) *Nat Genet* 25:139–140.
28. Wallace JL, MacNaughton WK, Morris GP, Beck PL (1989) *Gastroenterology* 96:29–36.
29. Ameho CK, Adjei AA, Harrison EK, Takeshita K, Morioka T, Arakaki Y, Ito E, Suzuki I, Kulkarni AD, Kawajiri A, Yamamoto S (1997) *Gut* 41:487–493.